http://mmg.tversu.ru ISSN 2311-1275

Mathematical Modelling and Geometry

Volume 2, No 2, p. 1 – 18 (2014)

Electron Spectrum, Localization and Tunneling in Double Nanoscale Structures

Igor Filikhin[a], **Sergei Matinyan and Branislav Vlahovic**

Department of Physics, North Carolina Central University, 1801 Fayetteville Street, Durham, NC 27707, USA

e-mail: [a] ifilikhin@nccu.edu

Received 26 March 2014. Published 4 May 2014.

Abstract. We study electron localization and tunneling in double quantum dots (DQD) and rings (DQR). The wave function of a single electron may be localized in one of the QDs or be delocalized when is spread over the whole system. Spectral distributions of such states are considered. Electron transition between both states is possible if inter-dot distance or QD (QR) geometry is varied. The effect of violation of symmetry of DQDs geometry on the tunneling is studied in details. We show that a small violation of symmetry drastically affects localization of electron. The same symmetry violation effect happens if an electrical or magnetic field are applied. We consider anti-crossing of the levels as the mechanism of the tunneling between the localized and delocalized states.

Keywords: quantum rings and dots, electron states, single-electron tunneling

PACS numbers: 73.21.-b, 73.21.La, 73.23.Hk

This work is supported by the NSF (HRD-0833184) and NASA (NNX09AV07A).

1. Introduction

Semiconductor heterostructures, such as quantum dots and rings are, due to their unique properties, of potential interest for development of new nano-devices [1, 2]. Some of these properties are related to the electron tunneling that occurs between the nano-sized systems. Here we will consider tunneling between double quantum dots (DQDs) and will show that the electron localized-delocalized states and the tunneling are highly sensitive on the violation of the geometrical symmetry of the DQD system. Generally, the relation between tunneling and chaos is an inalienable phenomenon in the meso- and nano world. Technology itself with its imperfection of shapes of quantum dots (QDs) and quantum rings (QRs) provides the chaotic behavior in the QD and QR, which has a strong influence on the charge transport and other properties [2]. The problem of quantum chaos in these objects has a relatively long history, just since it entered science and technology [3, 4, 5, 6, 7, 8] (for recent review see [9]). One of the main results of these studies is that chaotic phenomena sensitively depend on geometry and, first of all, on the symmetry of these objects. The second fundamental phenomenon characterizing the behaviour of these confined objects is the tunneling which expresses of the matter wave structure of quantum mechanics. The tunneling is well known from textbooks and best illustrated by an example of the barrier penetration in a double well potential [10, 11]. However, in the general sense, as applied to the confined nano-objects, tunneling is a dynamical by nature, and not a direct result of the existence of the potential barrier, it is the property of the wave function of the whole system [12]. The main feature of this so called dynamical tunneling is for example the energy barrier splitting of the degenerate pairs of level, when the coupling between objects due to their common wave function results in the forming two nearly degenerate eigenstates, which are the linear combinations of the wave functions of the isolated objects [13, 14]. In the present paper we consider the situation motivated by the experimental data for semiconductor InAs/GaAs QDs and QRs, and one of the goals of the present study is the above mentioned important phenomena, as applied to the isolated system of QDs (and QRs). As a result, we show that a small symmetry violation in DQDs may significantly reduce electron transport through the system.

2. Model

We consider isolated quantum dots and rings composed of InGaAs in a GaAs substrate. This heterostructure is modeled utilizing a ***kp***-perturbation single sub-band approach [15]. The problem is mathematically formulated by the Schrödinger equation in two (three) dimensions:

$$\left(\hat{H}_{kp} + V_c\left(r\right) + V_s\left(r\right)\right)\Psi\left(r\right) = E\Psi\left(r\right). \tag{1}$$

Here $\hat{H}_{kp}$ is the single band ***kp***-Hamiltonian operator $\hat{H}_{kp} = -\nabla\frac{\hbar^2}{2m^*}\nabla$, $m^*{=}m^*\left(r\right)$ is the electron effective mass which depends on the position of the electron, and

$V_c(r)$ is the band gap potential. $V_c(r) = 0$ inside the QD (QR), and is equal to V_c outside the QD (QR), where V_c is defined by the conduction band offset for the bulk. The band gap potential for the conduction band was chosen as V_c=0.594 eV. Bulk effective masses of InAs and GaAs are m_1^*=0.024m_0 and m_2^*=0.067m_0, respectively, where m_0 is the free electron mass. $V_s(r)$ is the effective potential simulating the strain effect, it has an attractive character and acts inside the volume of the QD [15]. The magnitude of the potential can be chosen to reproduce experimental data. For example, the magnitude of V_s for the conduction band chosen in Ref. [16] is 0.21 eV. This value was obtained to reproduce results of the 8-th band ***kp***-calculations of Ref. [17] for InAs/GaAs QD. The BenDaniel-Duke boundary conditions [18] are used on the interface of the material of QD and substrate.

One can separate the angle variable for case when shape of the QDs (QRs) has rotation symmetry. In polar coordinates the wave function is represented as

$$\Psi_{n,l}(\rho,\varphi) = \Phi_{n,l}(\rho)\, e^{il\varphi},$$

where $n = 1, 2, 3...$ are radial and $l = \pm 0, \pm 1, \pm 2, ...$ are orbital quantum numbers.

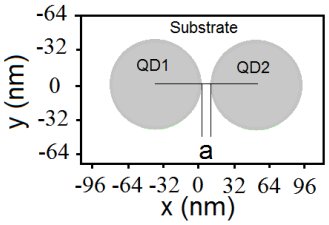

Figure 1: 2D circle shaped double quantum dot.

To describe the tunneling of a single electron in doublet quantum objects we make the following definitions. Probability of localization of electron into region Ω_γ (γ=1,2) is defined as $N_{k,\gamma} = \iint_{\Omega_\gamma} |\Phi_k(x,y)|^2 dxdy$, where $\Phi_k(\rho,z)$ is wave function of electron, $k = 1, 2, \ldots$ enumerates the levels in the spectrum. Ω_γ (γ=1,2) corresponds to the QD shape. Let us define a tunneling measure parameter $\sigma = \frac{N_{k,1}-N_{k,2}}{N_{k,1}+N_{k,2}}$, with the range [-1,1]. Obviously, when $\sigma = 0$, the electron will be in QD1 (Ω_1) or in QD2 (Ω_2) with equal probability (here we assume, that the QD1 and QD2 have the same shape). We will call this electron state the delocalized state of the electron in the double QDs system. The case $\sigma = 1$ (or $\sigma = -1$) corresponds to the strong localization of single election in QD1 (or QD2).

3. Identical QDs

The circle shaped InAs/GaAs dots compose the double quantum system. The DQD is considered as two dimensional (2D). The schematic of the system is given in Fig. 1. The inter-dot distance a is changed in this study.

Visualization for the dynamical tunneling is given in Fig. 2 where the parameter σ is presented along the energies of the single electron spectrum in the InAs/GaAs DQD for different inter-dot distances. When the distance between the objects is large, the electron is localized in one of the objects $\sigma \approx 1$ ($\sigma \approx -1$), when the distance decreases, the electron is tunneling and its wave function is spread over the whole double system, $\sigma \approx 0$. The situation when all states are tunneled states occurs for the inter-dot distances less than 15 nm. There are no tunneled states when a is larger than 40 nm. One can see in Fig. 2 that $\sigma = 0$ for a system that is symmetric relative to the axis, there are quasi quadruplets or quasi doublets of the DQD spectrum. The spectrum has degeneracy order of two for each level when the QDs are independent. This degeneracy follows from the rotation symmetry of each QDs. Energy of the states can be approximated by the relation: $E_{n,l} \sim \hbar^2/2\mathrm{m}^*(n + |l|)$, where n and l are radial and orbital quantum numbers. The states with σ between $|\sigma| = 1$ and $\sigma \approx 0$ are delocalized states. The example of wave functions of such states is shown in Fig. 3.

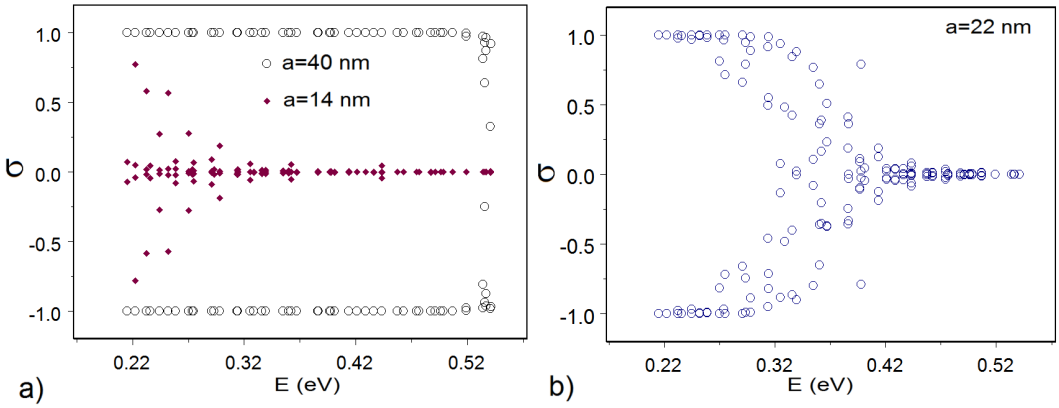

Figure 2: The parameter sigma for the confinement single electron states energies for InAs/GaAs DQD. Inter-dot distances a are a) 14 nm and 40 nm; b) 22 nm.

One can see that the two quasi doublets create the quadruplet, shown in left and right part of Fig. 3 (fig. 3 a),c) and b)d), respectively). In each quasi doublet the wave function has to be a symmetric Ψ^A or anti-symmetric Ψ^S w.r.t. the permutation of the left and right QDs. These quasi-doublets differ by the symmetry of the wave functions. The wave functions of the right side of Fig. 3 are "even" whereas the states of the left side are "odd". It can be described by an expansion of the *sin* or *cos* functions. The difference of the phase components of these wave functions can also be observed as a relative rotation for an angle $\vartheta = \pi/2l$. One can see that the wave functions of the quasi-doublet, Fig. 3 left, have different amplitudes for left and right QDs. Also, the wave functions have an additional rotation shift for small angles φ and $-\varphi$ relative to the "regular" position (see Fig. 3 b,d).

In the weak coupling state of the quasi-doublet, the wave function may be given

by the form [19]:

$$\Psi^A \approx -e^{-i\varphi}\frac{W}{2\Delta \mathrm{E}}\psi^L + \psi^R,$$

$$\Psi^S \approx \psi^L + e^{i\varphi}\frac{W}{2\Delta \mathrm{E}}\psi^R. \tag{2}$$

in the first order of $\frac{W}{\Delta E} << 1$, where $W \approx 0$ and $\Delta E \approx 0$. Here, W is a coupling coefficient depending on overlapping of the wave functions of "unperturbed states" ψ^L and ψ^R of the left (L) and right (R) quantum dots. $\Delta E = E^A - E^S$ is energy difference of the quasi-doublet.

One can explain the values of σ, with the condition $0 < |\sigma| < 1$ by Eq. (2). The levels located between states which are strongly tunneled (delocalized) and the states with no tunneling (localized) have values of σ as showed in Fig. 2. According to Eq. (2) the amplitudes of the wave function components corresponding to the left and right QDs differ for the factor $\frac{W}{\Delta E}$. The wave function components with smaller amplitudes have additional phase shift $\pm\varphi$. This situation is presented in Fig. 3a) and c).

It has to be noted that the numerical calculations for such states meet principal difficulties due to the necessity of numerical treatment of the uncertainty of the type 0/0 in Eq. (2) for the value $W/\Delta E$. Generally one can say that for identical QDs the tunneling goes consecutively from high energy levels to the ground state when the inter-dot distance is decreasing. Summarizing, we can mark the three parts of the spectrum: separated QDs part (localized levels), weak coupling part, and the strong coupling part (delocalized levels). Each level with $l \neq 0$ is a member of a quasi-quadruplet including two quasi doublets. The wave function components of the quasi-doublet can be distinguish by phase and amplitude for left and right QDs.

In Fig. 3, all levels of the spectrum are delocalized levels for the inter-dot distances of a <15 nm. The wave function of the electron is spread over whole DQD for each electron state. The quasi-doublet energy splitting ΔE can be described using the following relation (the consideration for one dimensional DQD one can find in [11]):

$$\Delta E \sim \sum \int \psi^L(x,y) V(x,y) \psi^R(x,y) dxdy, \tag{3}$$

where $V(x,y)$ is the confinement potential in the left or the right QD. The sum means a sum for two QDs. Here we assume that these wave functions were normalized. In considering quantum rings system, the result of this integration depends on an overlapping of the wave functions. This overlapping depends on the distance between quantum rings and spreading of the single wave function over the DQD geometry region. The last feature of the relation of Eq. (3) explains the spectral property of the dynamical tunneling mentioned above. The upper levels of the spectrum have more spaced wave functions. The value of the integral (3) is larger for the upper levels in comparison with one for the low-lying levels.

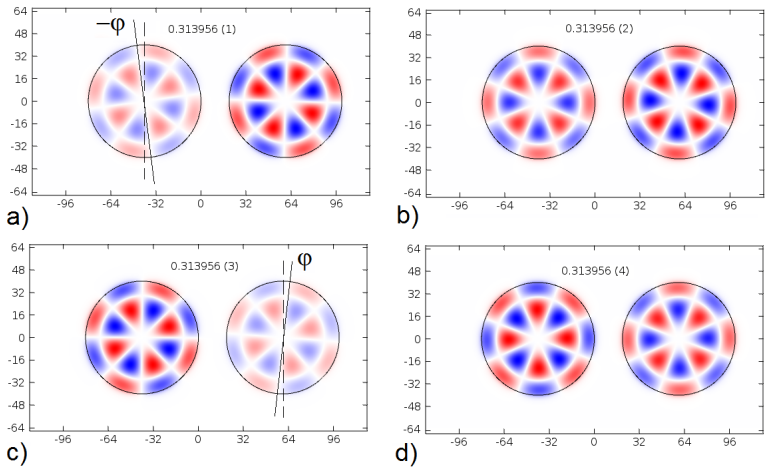

Figure 3: The wave functions of quasi quadruplet state with energy of 0.313956 eV. The inter-dot distance is a=15 nm. Two quasi doublets create this quadruplet (shown by number 1,3 and 2,4)

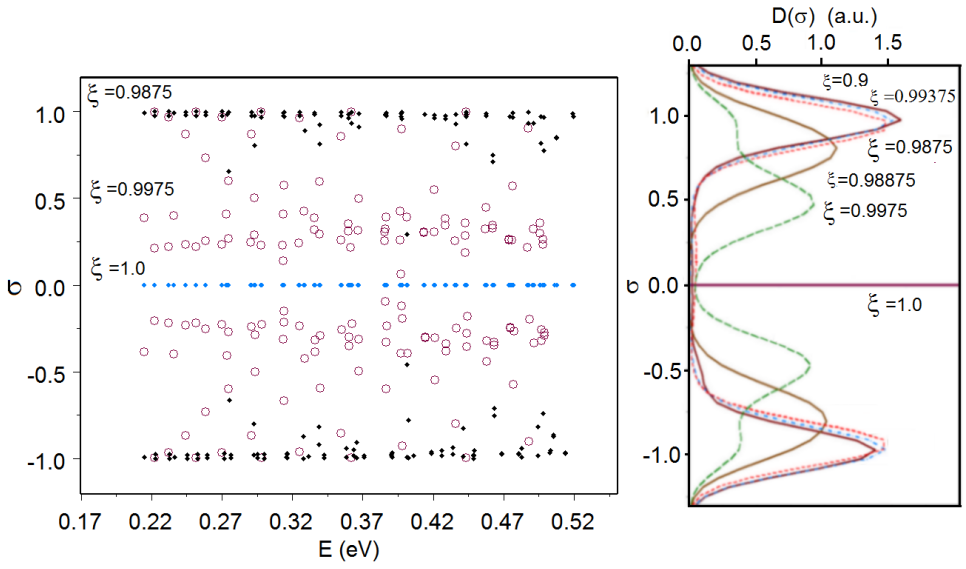

Figure 4: a) Parameter σ for different coefficient of asymmetry in DQD with R_1=40 nm and $R_2 = \xi R_1$ for a=3 nm. b) Density functions of the σ parameter for different ξ.

4. Non-identical QDs

Let us consider non-identical DQDs. Note that the similar consideration has been done in Ref. [14] for a micro-disk. We take initial radii of the QDs 40 nm. The size of one of the QDs (right QD) is gradually decreased. The inter-dot distance was kept with the value of 3 nm. The effect of non-identicalness on the tunneling parameter is seen in Fig. 4a). We used ratio $\xi = R_2/R_1$ of the radii of the QDs for defining the non-identicalness.

The cases $\xi = 1$, $\xi = 0.9975$ and $\xi = 0.9875$ are compared in Fig. 4 a). One can see that when $\xi = 1$ the wave function is distributed uniformly between QDs, when $\xi = 0.9975$ there are few states of single electron whose wave functions are well localized in the left or right QDs. For $\xi = 0.9875$ all states have strong localization in the left or right QDs. The efficiency of tunneling depends on the ratio of asymmetry of QDs shapes. The larger asymmetry gives larger number of non-tunneled states. It is important to note that the small violation of the QD symmetry drastically affects the tunneling. In Fig. 4b) the last result is presented using the density functions $D(\sigma)$ of σ shown for various ξ. The function $D(\sigma)$ is defined as a probability density for the variable σ to have a value σ with the normalization $\int D(\sigma)d\sigma = 1$. We see that the separation of the electron spectral states between two cases – "independent QDs" (no tunneling states) and "completely coupled QD" occurs for ξ in vicinity of 1.

One more illustration for the effect is given in Fig. 5 where we show the effect of the DQD asymmetry, when the DQs are separated by relatively large distance a=10 nm. All states of the DQD are tunneling states for identical QDs for that distance. The tunneling of the system drastically decreases with small variations of the right QD radius.

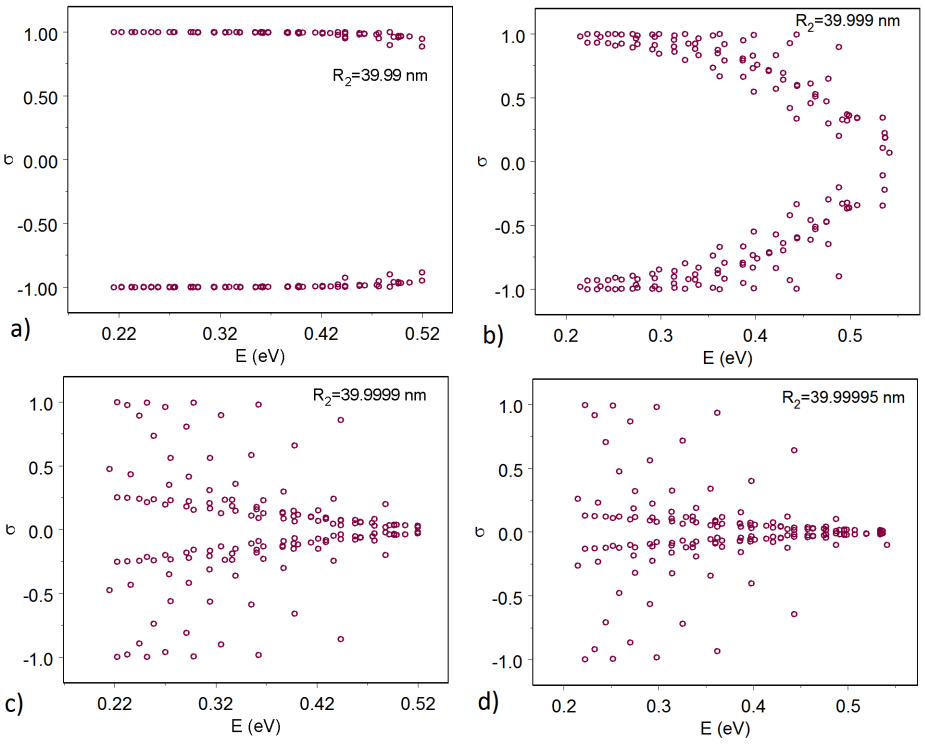

Figure 5: The σ-parameter for the asymmetric DQD with a=10 nm for several values of the asymmetry parameter $\xi = R_2/R_1$ (R_1=40 nm): a) ξ=0.99975 ; b) ξ=0.999975. c) ξ=0.9999975. d) ξ=0.99999875. The corresponding values of R_2 are shown in the figures. For all cases, the relative deference of QD shape square areas is less than 0.05%.

In Fig. 6 and Fig. 7 the dependence of the tunneling on inter-dot distance is demonstrated. In Fig. 6 the violation of the symmetry of this DQD system, defined by ξ, is 0.9975. Comparing the cases of symmetric (see Fig. 2) and non-symmetric DQD tunneling one can see that for symmetric case all states in the spectrum are delocalized, when the distances decrease from a=10 nm to a=0. In the case of non-symmetric DQD there are some localized states for any a up to a=0.

Note also that the inter-dot distance value, for which all states of the DQD spectrum are tunneled, essentially depends on value of ξ. For non-symmetric DQD this inter-dot distance decreases to a few nm while for the identical QDs this distance is about 10 nm. Thus, we can conclude that a violation of symmetry of the DQD geometry reduces the tunneling.

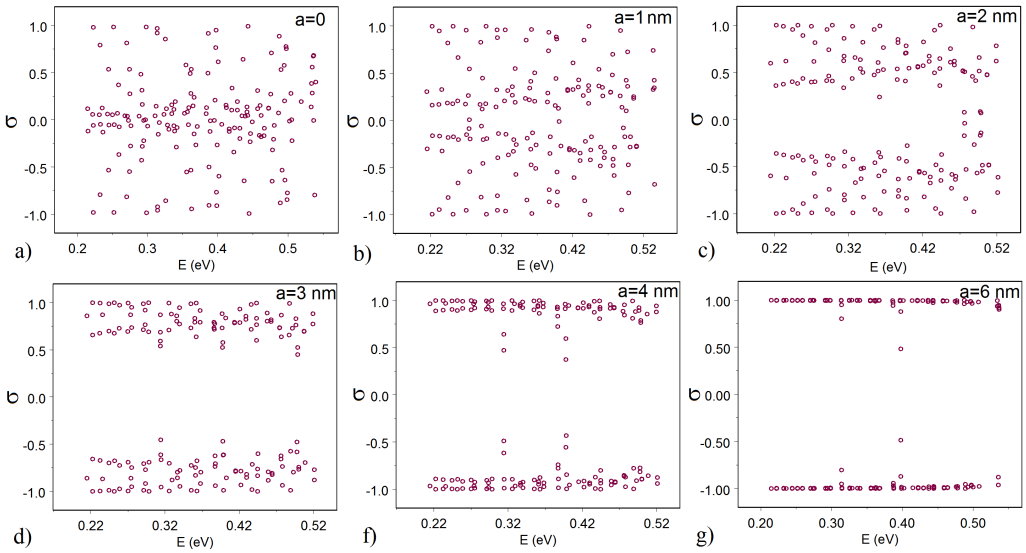

Figure 6: The σ-parameter for the asymmetric DQDs with R_1=40 nm and R_2=39.9 nm, for different inter-dot distances a.

An additional illustration for this conclusion is presented in Fig. 7, where we compare the tunneling for two cases: small (with ξ=0.9975) and relatively large (with ξ=0.875) asymmetry in DQDs. Obviously, number of the delocalized levels (and the tunneling) is larger for the case of small asymmetry.

5. InAs/GaAs DQD in 3D

In this section we consider the DQDs with the geometry motivated by the experimental data. The reported geometry parameters for QD in [1] have the value about 20 nm for QDs diameter and the value of 9 nm for QDs height. The cross section of the DQDs shape is shown in Fig. 8a (see also [20]).

First, we consider the case of identical QDs in DQDs. The value of QDs diameter was chosen to be larger that the reported in [1]. To have a large number of

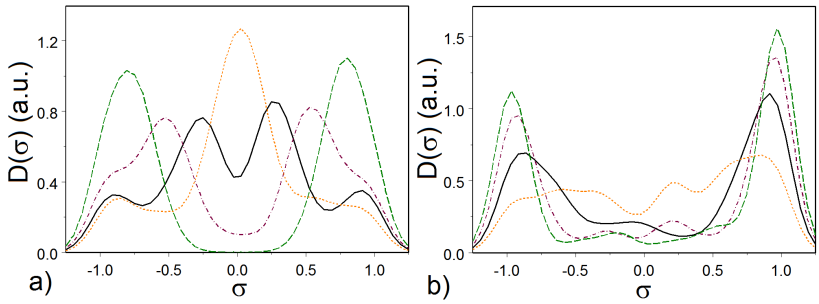

Figure 7: Density function of σ for different inter-dot distances a for the asymmetric DQDs with a) R_1=40 nm and R_2=39.9 nm and b) R_1=40 nm (ξ=0.9975) and R_2=35.0 nm (ξ=0.875). Dashed line - a=3 nm; dot-dashed line - a=2 nm; solid line - a=1 nm; doted line -a=0 nm.

confinement states (about one hundred), we increased the QDs size. The results of the calculations are presented in Fig. 8b).

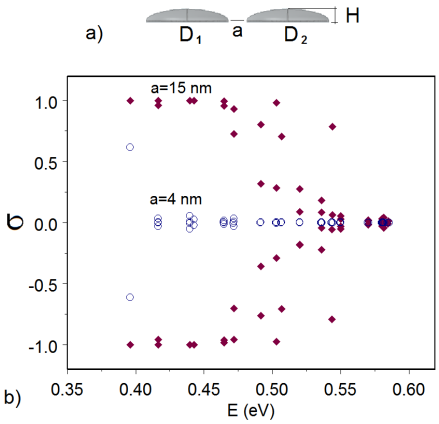

Figure 8: a) Cross section of 3D semi-ellipsoidal shaped DQDs. b) σ-parameter for 3D InGaAs/GaAs DQDs with R_1=R_2=20 nm calculated for energies of single electron spectrum for different inter-dot distances a (shown in the figure).

These results are qualitatively the same as ones obtained for 2D QD in previous section: if we make the QDs closer, then the tunneling involves consequently the levels from the higher to the lower. The tunneling of high levels begins at 24 nm. The system becomes completely delocalized when the inter-dot distance is about 4 nm. The 3D and 2D DQDs systems are different in the respect that the distances for the 3D DQDs at which the full tunneling occurs are shorter. For these examples the difference is larger four times: from the value of 16 nm for 2D DQD to the one of 4 nm for 3D DQD.

This effect could be expanded by including into account the case of non-identical QDs in DQDs. We have chosen for the left QD radius 20 nm and the right QD radius about 19 nm (ξ=0.95). We changed only the size area of basis of the QD

shape. The heights of the QD ware not changed. Difference of the volumes is about 10% (ξ^2=0.9). For the situation when the inter-dot distance decreases to zero we found that in this DQD system the tunneling is never over the whole system (if QDs do not penetrate one into another). Comparing regular DQDs and asymmetric DQDs considered above one can conclude again that a violation of the symmetry in DQDs leads to reduction of the tunneling.

6. Lateral double quantum rings with concentric symmetry violation

Let us consider the laterally arranged DQRs, likewise DQDs considered above. The DQRs of such type are shown in Fig. 9 (left). Here, Δx is the shift of inner circle in upper QR that breaks concentric symmetry of this ring. This case is interesting since the symmetry of this double quantum object could be violated without the QR shape volume change. Note that the upper QR is shaped like "chaotic Bohigas billiard" [21].

Energy of a single electron in "regular" QR is related through the following relation to the radial n and orbital quantum number l:

$$E_{n,l}\sim\hbar^2/2\mathrm{m}^*(n^2/W^2+l^2/R^2),$$

where $W<<R$ and W is the width and R is radius of the QR. One may use for R the value $(r_{in}+r_{out})/2$, where r_{in} and r_{out} are radii of inner and outer boundary circles of QR. The single electron levels in QR are separated by the bands n=1,2,3 ..., and in-band states by $|l|$=0,1,2.... Since $W<<R$, the density function $D(E)$ of the electron energy spectrum has local maximums for the beginning of each n-band n =1,2,3,.... The maximums are presented in Fig. 9a) for the regular case Δx=0. The tunneling spectral distribution is similar to that of the DQDs; the number of the delocalized states consecutively decreases from the threshold of the continuous spectrum. The violation of the symmetry occurs when the eccentricity $\Delta x \neq 0$. The upper ring (QR2) becomes "chaotic" [22]. The spectrum of the QR is splitted into the n-bands as it is shown in Fig. 10.

For large orbital numbers l the wave functions of the electron are localized in the area corresponding to the regular ring, which outer boundary is given in Fig. 10 by red circle. These electron states build so called "whispering gallery" [21] (shown by red filled circles in Fig. 10 for n=1). The wave functions of these sates in chaotic QR are similar (asymptotically for large l) to the ones in regular QR with radius slightly bigger than one in "non-disturbed" initial QR. This situation is shown by red circle in Fig. 10 inset. Using these definitions we can clarify Fig. 9b)-d). The delocalized tunneling between chaotic QR (QR2) and regular QR (QR1) is possible through the gallery states of QR2 with the same orbital number l. The number is larger than the number l_{wg} that corresponds to the "gallery", when the spectral levels become the "gallery" states. The non-gallery states have no "good" orbital quantum number and the tunneling between QR1 and QR2 is suppressed. We

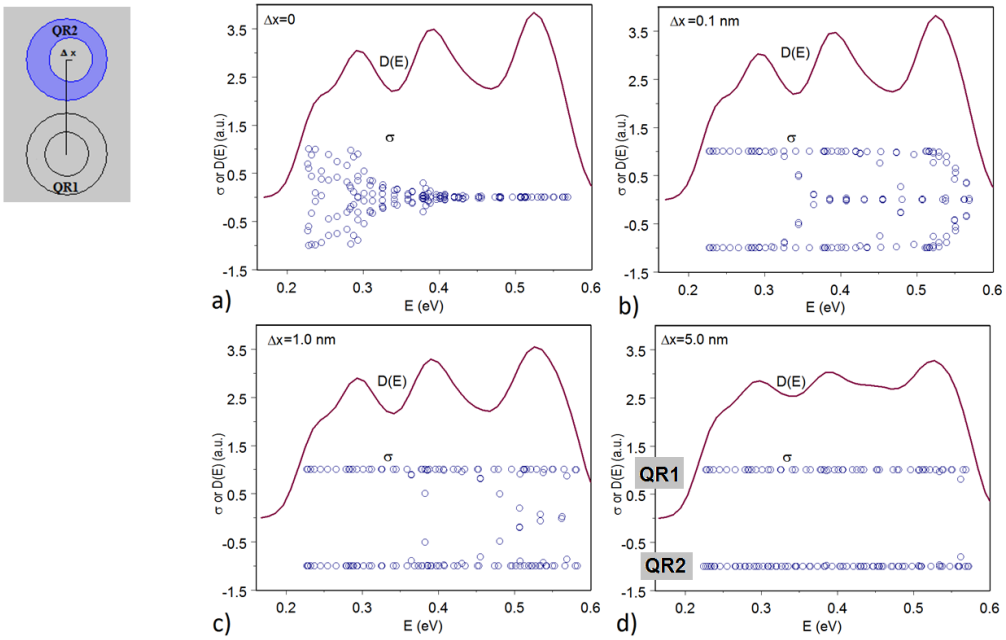

Figure 9: (left) The laterally disposed QRs in DQR. Δx is the shift of inner circle in upper QR. (right) σ-parameter and density function $D(E)$ of energy levels along the DQR spectrum.

can see in Fig. 9b)-c) that the delocalized states are appearing at large l, for the states with the radial numbers n=1,2. The tunneling is also suppressed when Δx became large enough, as it is shown in Fig. 9d). This situation can be explained by a shifting the "gallery" states to the continue spectrum threshold when the asymmetry increases (see [22]). In another words, there are no "gallery" states in the QR2 spectrum with this value of Δx.

7. InAs/GaAs double concentric quantum rings

The double concentric quantum ring is an example of the double quantum object with non-identical parts. It is clear for the same heights of the outer and inner rings, that the volume area of the inner and outer rings are different (we consider comparable widths for the rings). Tunneling in such DQR occurs through the levels with the same symmetry due to the level anti-crossing [23]. The electron localization in the inner ring corresponds to σ about 1 and the outer ring localization - with σ about -1. In Fig. 10, we show results of the calculations which can be presented as "traces" for each radial number n=1,2,3. The tunneling in DQRs occurs between the levels having the same type of wave function symmetry defined by the orbital quantum number l. For these states the tunneling is possible through the anti-crossing mechanism [23].

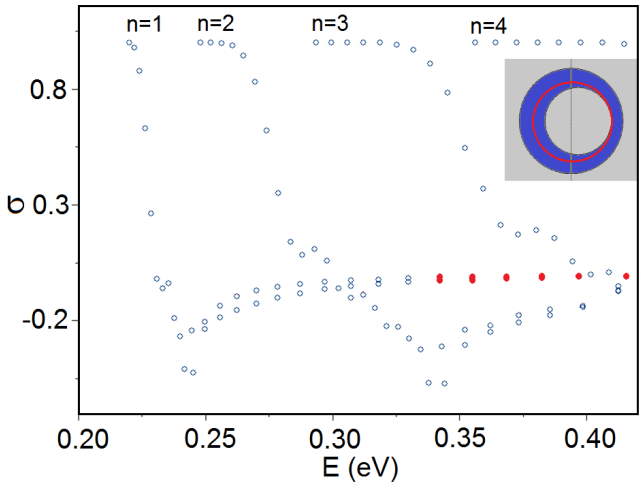

Figure 10: σ-parameter along the chaotic QR spectrum. The numbers mark the beginning of each n-band. The red filled circles correspond to the "gallery" states. (inset) The shape of the chaotic QR is shown by blue. The red circle means the inner boundary of the wave function localization area of the "gallery" states, which appears at large values of the orbital numbers l.

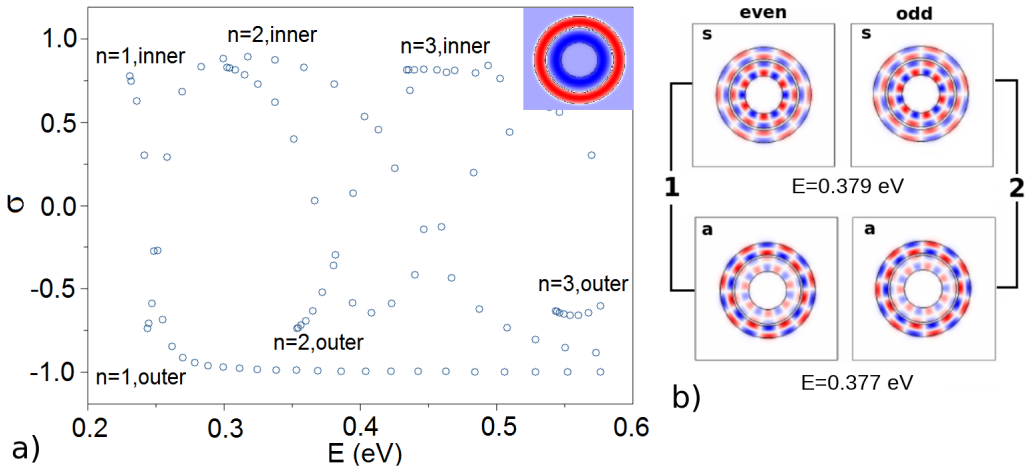

Figure 11: The parameter σ for spectrum of InAs/GaAs concentric DQR. The radial quantum numbers of the each ring are given for "independent rings". The calculated points, connected in order of increasing l=1,2,3,... for each n-band, noted by "traces". The concentric DQR shape is shown in inset: the blue is inner ring and the red is outer ring. Geometry parameters are R_1=30 nm, R_2=40 nm for outer ring; R_1=16 nm. R_2=28 nm for inner ring. The inter-ring distance is 2 nm (the geometry was scaled by factor 1.5 for the calculations).

8. Violation of the symmetry in DQD and QR under homogeneous electric field

In the previous sections we considered the tunneling effect related to the violation of the shape symmetry of DQDs. Here we show that the effect of the violation of the symmetry can be replaced by the effect of the external electric potential, which depends on the coordinate of the electron (see also [24]).

The lateral electric filed F adds the potential $V_e = eFx$ in the Hamiltonian of the system. The QDs are considered to be directed along the x-axis. The electron confinement becomes different in the left and right QDs after switching on an electric field, as it is presented in Fig. 11a) schematically.

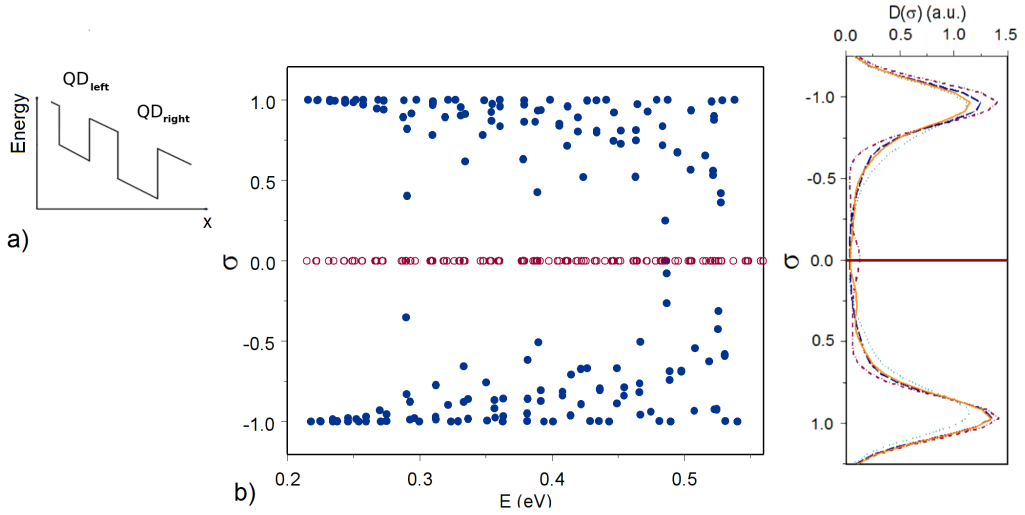

Figure 12: a) Electron confinement of DQD in the electric field; b)(left) The σ-parameter of the single electron states in InAs/GaAs DQD. Open circles (solid circles) correspond to the calculated results without electric filed (with the electric field F=0.25 (kV/cm)); (right) Density functions $D(\sigma)$ of the σ-parameter are shown for different values of the electric field. Dot-dashed curve is the result with F=1 (kV/cm), dashed curve - with F=4 (kV/cm), solid line - with F=0, doted curve - F=0.25 (kV/cm). Inter-dot distance is a=2 nm; QD radii are 40 nm.

We consider two versions for the DQD geometry. In the first one, QDs in the system are identical (radius of each QD is 40 nm). The inter-dot distance a is fixed in this study. Visualization of spectral properties of the tunneling is given in Fig. 12 where the parameter σ is presented along the energies of single electron spectrum in the InAs/GaAs DQD without the electric field and with weak electric field (F=0.25 kV/cm). In the first case there are no states localized exactly in one or other QD due to relatively small inter-dot distance (a=2 nm), all states are "delocalized". In the second case, there are a number of strong localized states. The system looks as "mostly separated" for the electron motion. One can see from Fig. 12 that weak electric field effects drastically affect the tunneling properties of

the system (see also [25]), for the whole spectrum. In Fig. 12b) the density functions $D(\sigma)$ of the σ-parameter are shown for different values of the electric field. The maximums of the density $D(\sigma)$ corresponds to the most probable localization of the electron in one of the QDs (left or right). The horizontal line corresponds to $D(\sigma)$ with no electric field, when the density function is δ-function. It is important to note that the decreasing of the field magnitude does not change the situation of the tunneling.

The case of non-identical QDs is more interesting because it better corresponds to the experimental practice. In the system of non-identical QDs, these characteristic distances decreased essentially to a few nanometers, depending on the value of the violation of the QD shape symmetry. For the DQD placed in a longitudinal electric filed the reduction of the tunneling also occurs. In the x direction, the symmetry of the corresponding quantum wells is violated. The effect of the electric field to the electron tunneling is visible when $\xi \approx 1$. The results of such calculations for the density functions $D(\sigma)$, for different values of the electric field, when ξ=0.9975 are presented in Fig. 13. There are two peaks for $\sigma \approx$1 and $\sigma \approx$-1. In other words, the electric field "delocalizes" electron wave function and reduces electron transport through the system.

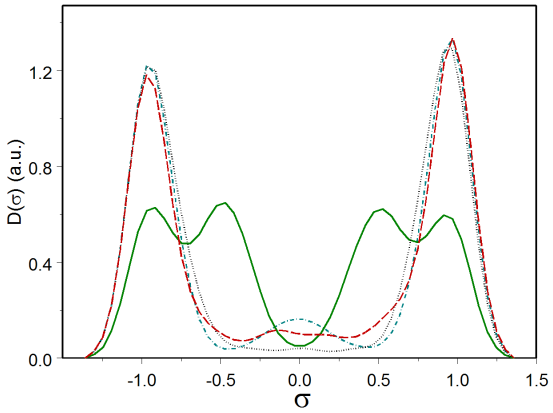

Figure 13: Density functions $D(\sigma)$ of the σ-parameter are shown for different values of the electric field for ξ=0.9975 (R_1 =40 nm, R_2 =39.9 nm). All notations are the same as in Fig. 12b.

9. Electron transition in DQD and DQR in magnetic and electric fields: level anti-crossing

We can rule the localized-delocalized tunneling using the magnetic of electric fields. The electron transition between parts of double quantum object can be occur in such situation. The InAs/GaAs concentric DQR located in the perpendicular magnetic field is modeled in our work [23]. We assume that the QRs are weakly coupled in this complex. It means that there are no delocalized states when the magnetic field

is zero. In non-zero field the levels with $-l$ and l are separated due to the Zeeman effect. Because the rings have different radii, it is possible that the levels of the weak coupled rings is crossed when the magnetic field is increasing. The levels with equal orbital number (and the same symmetry) may be anti-crossed (see also [14]). The anti-crossing is accompanied by delocalization of electron wave function.

The same mechanism of the tunneling can be obtained in the system of non-identical QDs located in the lateral electric field. Effect of electron transition take the place also in this case. This situation is shown in Fig. 14. The anti-crossing of the levels in increasing electric filed is presented in Fig. 14a). The transition of the electron is occurred when the electric field F reaches a value about 2.2 kV/cm. The wave function localized initially on the right QD becomes to be delocalized. Increasing electric filed changes the state to localized one in the left QD.

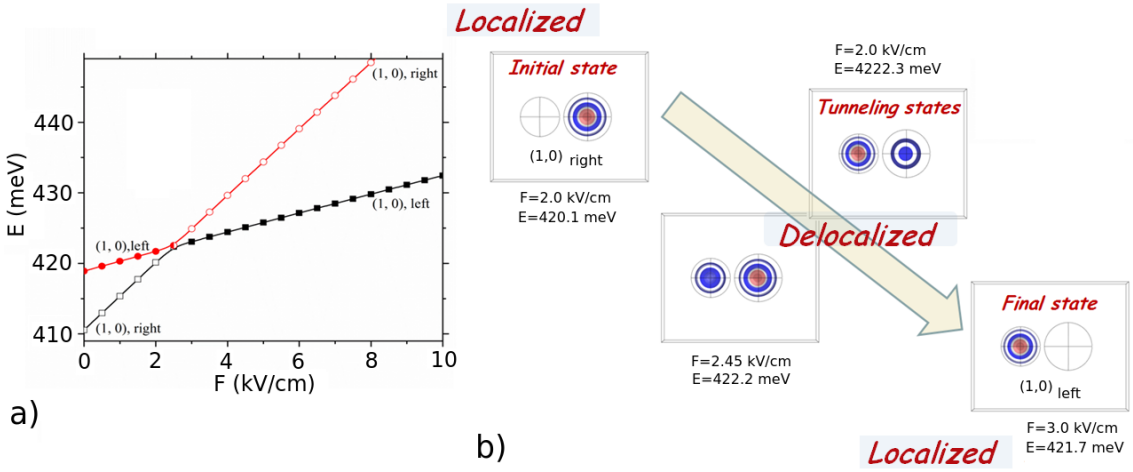

Figure 14: a) Single electron energy of DQD in lateral electric field F. Anti-crossing of the levels $(1,0)_{left}$ and $(1,0)_{rigth}$, where (n,l) mentions the set of the redial and orbital quantum numbers, are shown. QDs have semi-ellipsoidal shape with the diameters D_1=28 nm and D_2=34 nm, high H =8 nm and inter-dot distance S =3 nm. b) Transition of electron between right and left QDs under increasing electric field F. The wave functions of the electron are shown for the initial, tunneling and final states. The energies E of the states are given.

10 Conclusions

We studied dynamics of localized-delocalized states of electron spectrum in the DQDs and DQRs with the respect to the nanostructure geometry. The two types of the tunneling are found that correspond to the DQDs composed from identical and non-identical QDs. The violation of the symmetry of the DQD geometry diminishes the tunneling. The violation of the symmetry can be caused by a geometry deformation or by external fields. We show that the electron states with the same

type of rotation symmetry play important role for the tunneling in the DQDs and DQRs due to the level anti-crossing mechanism. High sensitivity of the tunneling to the geometry change can be technologically important.
This work is supported by the NSF (HRD-0833184) and NASA (NNX09AV07A).

References

[1] Lorke A., Luyken R. J., Govorov A. O., and Kotthaus J. P., *Spectroscopy of Nanoscopic Semiconductor Rings*, Phys. Rev. Lett. 2000, **84**, pp. 2223-2226

[2] Ponomarenko L.A., Scheidin F., Katsnelson M.I., Yang R., Hill E.W., Novoselov K.S., Geim A.K.,*Chaotic Dirac Billiard in Graphene Quantum Dots.* Science 2008, **320**, pp. 356-358

[3] Baranger H.U. and Stone A.D., *Quenching of the Hall resistance in ballistic microstructures: A collimation effect.* Phys. Rev. Lett. 198,9 **63**, pp. 414-417

[4] Beenakker C.W.J. and van Hoiten H., *Billiard model of a ballistic multiprobe conductor.* Phys. Rev. Lett. 1989, **63**, pp. 1857-1860

[5] Whitney R.S., Schomerus H., Kopp M., *Semiclassical transport in nearly symmetric quantum dots. I. Symmetry breaking in the dot*, Phys. Rev. E 2009, **80**, pp. 056209-16; Whitney R.S., Marconcini P., Macucci M., *Huge Conductance Peak Caused by Symmetry in Double Quantum Dots*, Phys. Rev. Lett. 2009, **102**, pp. 186802-4

[6] Nazmitdinov R. G., Sim H.-S., Schomerus H., and Rotter I., *Shot noise and transport in small quantum cavities with large openings*, Phys. Rev. B 2002, **66**, pp. 241302R-4

[7] Filikhin I., Matinyan S., Schmid B.K. and Vlahovic B.,*Vlahovic, Electronic and level statistics properties of Si/SiO2 quantum dots*, Physica E 2010, **42**, pp. 1979-1983

[8] Filikhin I., Matinyan S. and Vlahovic B., *Disappearance of quantum chaos in coupled chaotic quantum dots*, Phys. Lett. A 2011, **375**, pp. 620-623

[9] Filikhin I., Matinyan S. G., and Vlahovic B., *Quantum Mechanics of Semiconductor Quantum Dots and Rings*, published as a chapter in Fingerprints in the Optical and Transport Properties of Quantum Dots, ed. Ameenah Al-Ahmadi, (InTech, 2012) 468 pp.

[10] Manasreh O., *Semiconductor Heterojunctions and Nanostructures* (Nanoscience & Technology), McGraw-Hill, New York (2005), 554 pp.

[11] Bastard G., *Wave Mechanics Applied to Semiconductor Heterostructures* (Halsted Press, 1988).

[12] Davis M.J., Heller E., *Quantum dynamical tunneling in bound states*, J. Chem. Phys. 1981 **75**, pp. 246-254

[13] Rotter I. and Sadreev A. F., *Avoided level crossings, diabolic points, and branch points in the complex plane in an open double quantum dot*, Phys. Rev. E 2005, **71**, pp. 036227-14

[14] Ryu J.-W., Lee S.-Y., and Kim S. W., *Coupled nonidentical microdisks: Avoided crossing of energy levels and unidirectional far-field emission*, Phys. Rev. A 2009, **79**, pp. 053858-7

[15] Filikhin I., Suslov V. M. and Vlahovic B., *Modeling of InAs/GaAs quantum ring capacitance spectroscopy in the nonparabolic approximation*, Phys. Rev. B 2006, **73**, 205332, 4pp.

[16] Filikhin I., Suslov V. M., Wu M. and Vlahovic B., *InGaAs/GaAsquantumdots within an effective approach*, Physica E 2009, **41**, 1358-1363

[17] Schliwa A., Winkelnkemper M. and Bimberg D., *Impact of size, shape, and composition on piezoelectric effects and electronic properties of In(Ga)As/GaAs quantum dots*, Phys. Rev. B 2007, **76**, pp. 205324-17

[18] BenDanel D. J., Duke C. B., *Space-Charge Effects on Electron Tunneling*. Phys. Rev. 1966, **152**, pp. 683-693

[19] Cohen-Tannoudji C. , Diu B., Laloë F., *Quantum Mechanics*, Volume 1, 1978

[20] A. A. Gusev, O. Chuluunbaatar, L. L. Hai, S. I. Vinitsky, E. M. Kazaryan, H. A. Sarkisyan and V. L. Derbov, *Spectral and optical characteristics of spheroidal quantum dots*, Journal of Physics: conference series, 2012, **393**, pp. 012011-9

[21] Bohigas O., Boose D., Egydio de Carvallho R., and Marvulle V. *Quantum tunneling and chaotic dynamics*. Phys. A 1993, **560**, pp. 197-210

[22] Filikhin I., Matinyan S. G., Vlahovic B., *Electron tunneling in chaotic InAs/GaAs quantum ring*, will be appeared in *Quantum Matter*; arXiv:1211.1991

[23] Filikhin I., Matinyan S. G., and Vlahovic B., *Electron trapping in weakly coupled concentric quantum rings*. Quantum Computers and Computing 2011, **11**, pp. 35-43; Filikhin I., Matinyan S., Nimmo J., Vlahovic B., *Electron transfer between weakly coupled concentric quantum rings*. Physica E 2011, **43**, pp. 1669-1676

[24] van der Wiel W.G., De Franceschi S., Elzerman J.M., Fujisawa T., Tarucha S., Kouwenhoven L.P., *Electron transport through double quantum dots*. Rev. Mod. Phys. 2003 **75**, pp. 1-22

[25] Bleibaum O., Belitz D., *Weak localization of electrons in an external electric field*, Phys. Rev. B 2004, **69**, pp. 075119-10